Supporting Information for:
Secondary organic aerosol formation from biomass burning emissions

Christopher Y. Lim, David H. Hagan, Christopher C. Cappa, Matthew M. Coggon, Abigail R. Koss, Kanako Sekimoto, Joost de Gouw, Carsten Warneke, Jesse H. Kroll

T1. Initial PM composition

Fire	Fuel	Included in analysis?	Sampling time (min)	Initial gas phase composition		Initial particle phase composition				
				NMOGs (ppb)	NMOG ($\mu g\,C\,m^{-3}$)	POA ($\mu g\,m^{-3}$)	BC ($\mu g\,m^{-3}$)	Org/rBC	O/C	H/C
Fire08	Engelmann spruce(PIEN)	Yes	15.00	250.06	369.75	51.80	0.76	216.00	0.33	1.79
Fire21	lodgepole pine (PICO) - Litter	Yes	11.32	167.14	261.53	28.83	2.29	33.89	0.25	1.84
Fire23	Subalpine fir (ABLA), Fish Lake - Canopy	No	5.13	183.49	263.15	9.66	18.36	1.41	0.45	1.70
Fire25	Engelmann spruce (PIEN) - Canopy	Yes	5.70	113.52	172.47	9.66	2.75	11.78	0.34	1.80
Fire26	Engelmann spruce (PIEN) - Duff	Yes	20.53	295.42	397.01	20.14	0.00	1300.93	0.20	1.86
Fire28	chaparral (manzanita) - Uncontaminated (M-NM), Canopy	Yes	7.28	456.18	680.61	46.14	24.00	4.91	0.27	1.79
Fire29	chaparral (chamise) - Contaminated (C-SD), Canopy	No	3.68	239.44	287.26	16.92	39.98	1.42	0.46	1.73
Fire30	chaparral (manzanita) - Contaminated (M-SD), Canopy	Yes	9.03	797.37	1055.01	68.13	43.74	5.15	0.32	1.75
Fire31	Douglas-fir (PSME), Rotten Log	Yes	18.95	768.22	1078.06	152.92	0.04	2836.27	0.60	1.79
Fire32	chaparral (chamise) - Uncontaminated (C-NM), Canopy	No	7.07	432.51	508.05	25.77	36.85	2.09	0.40	1.75
Fire33	chaparral (manzanita) - Contaminated (M-SD), Canopy	Yes	12.70	666.90	839.08	54.33	30.04	5.19	0.31	1.77
Fire38	ponderosa pine (PIPO) - Litter	Yes	7.70	196.89	297.53	19.12	5.00	8.16	0.34	1.78
Fire39	ponderosa pine (PIPO) - Canopy	Yes	13.02	635.94	1035.87	139.41	5.82	97.92	0.31	1.75
Fire41	lodgepole (PICO) - Litter	Yes	9.65	151.83	251.55	14.55	0.36	94.86	0.38	1.76
Fire43	Douglas-fir (PSME) - Litter	No	7.78	104.67	178.01	3.41	7.91	0.92	0.42	1.61
Fire46	chaparral (chamise) - Contaminated (C-SD), Canopy	No	8.22	246.90	347.08	13.89	32.64	1.26	0.50	1.68
Fire49	Excelsior	No	3.47	230.94	345.55	14.47	30.17	1.08	0.58	1.71
Fire50	Dung	Yes	19.50	955.79	1293.72	200.81	0.77	620.45	0.21	1.84
Fire51	Subalpine fir (ABLA), Fish Lake - Litter	No	9.97	158.29	284.58	9.07	10.87	1.47	0.26	1.78
Fire52	Engelmann spruce (PIEN)	Yes	16.90	227.36	331.91	24.82	4.14	17.86	0.38	1.73
Fire53	loblolly pine (PITA) - Litter	Yes	12.87	265.07	461.89	41.58	9.39	11.14	0.33	1.78
Fire56	Subalpine fir (ABLA), Fish Lake - Duff	Yes	16.12	632.51	927.77	28.70	0.02	1416.60	0.24	1.80
Fire57	Douglas-fir (PSME)	Yes	15.63	445.64	651.54	68.33	8.09	23.29	0.44	1.74
Fire61	Excelsior	Yes	7.47	480.06	687.78	33.90	26.87	3.46	0.52	1.73
Fire62	Bear Grass	Yes	14.25	546.89	771.58	67.12	3.93	115.32	0.32	1.74
Fire63	lodgepole (PICO)	Yes*	14.77	590.09	883.59	96.97	9.57	41.41	0.37	1.75
Fire64	Douglas-fir (PSME) - Canopy	Yes	11.93	1139.78	1731.36	194.96	6.04	212.28	0.37	1.72
Fire66	Sage	Yes	6.38	502.32	715.94	37.72	7.19	23.49	0.38	1.73

Table T1. Initial conditions in chamber for all PTR-ToF-MS and AMS measured experiments before start of oxidation. Fire 63 is a dark, control experiment (no oxidation). Fires with initial Org/rBC < 3.4 were excluded from the analysis presented in the paper due to enhanced wall loss from 254 nm light (see main text, Sect. 3.1).

T2. SOA carbon yields

	CE corrected		CE = 1
Days	**Yield**	**Standard error (1σ)**	**Yield**
0.25	0.24	0.04	0.04
0.5	0.32	0.05	0.07
1	0.38	0.06	0.09
2	0.44	0.09	0.10
3	0.51	0.09	0.12
4	0.56	0.09	0.14

Table T2. Table of SOA carbon yields from NMOG carbon reacted using CE correction presented in the text and assuming a constant CE equal to 1. NMOG carbon reacted is calculated based on initial NMOG concentration, OH exposure, and an average OH reaction rate constant based on identified NMOGs.

S1. Experimental setup
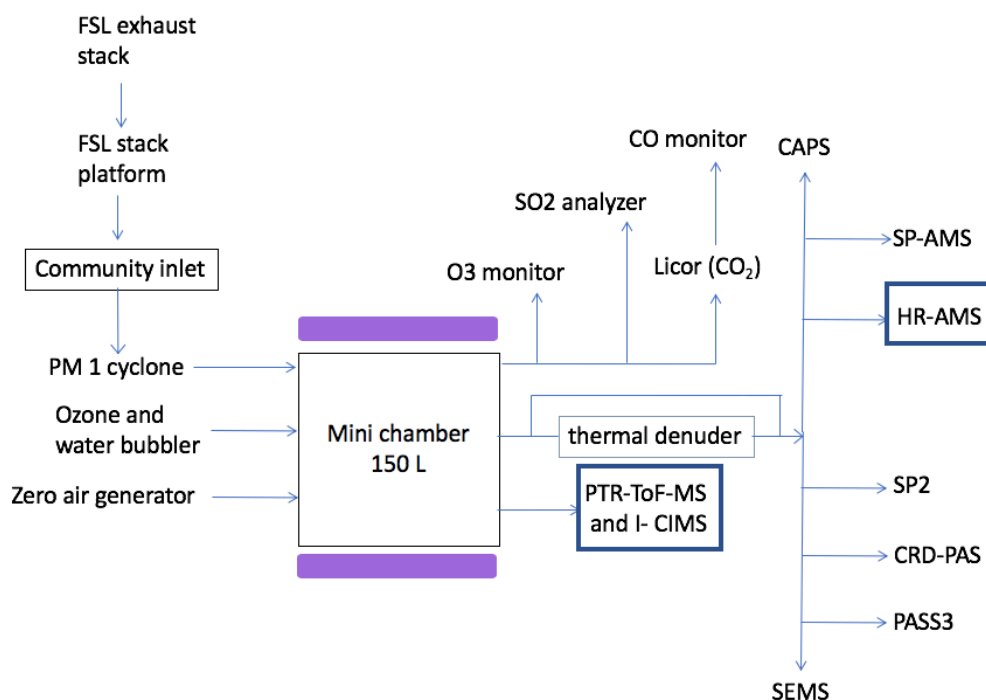
Figure S1. Experimental setup. Emissions from fires entered the exhaust stack and were drawn through a community inlet to the mini-chamber. Chamber was run in semi-batch mode. Full suite of instruments is shown.

S2. Comparison between stack and chamber
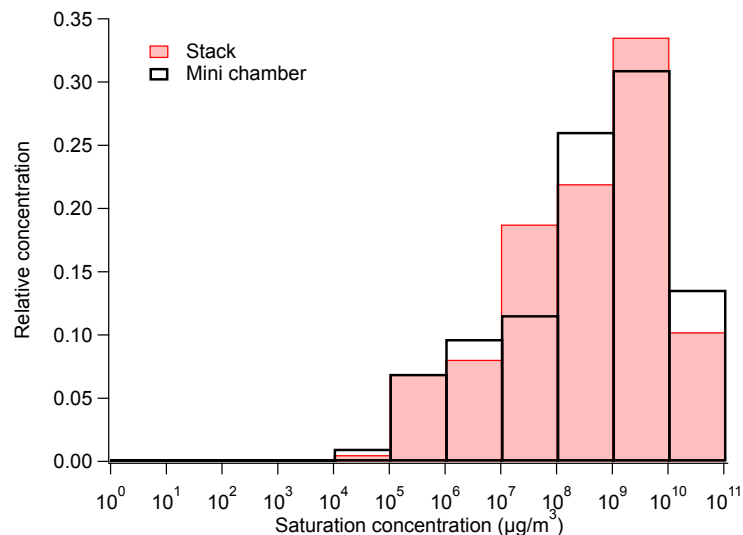
Figure S2. Comparison of volatility distributions for gas phase compounds measured in the mini chamber (black) and measured directly from the FSL stack in red (Koss et al., 2017). Distribution of compounds measured is roughly the same indicating that vapor losses from the community inlet or other transfer lines did not significantly affect the mixture of gas phase compounds entering the mini chamber.

S3. Collection efficiency parameterization
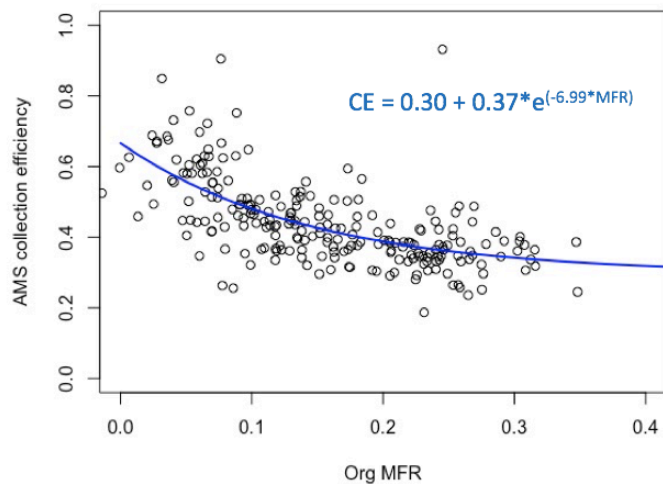
Figure S3. Calculated AMS collection efficiency vs. Org MFR (mass fraction remaining after passing through thermal denuder). Blue exponential fit (CE$_{best}$) was used to parameterize AMS collection efficiency correction for all data points. Red exponential fit (CE$_{max}$) was used to constrain the range of reasonable carbon yields in Fig. 6.

S4. OA wall loss fit
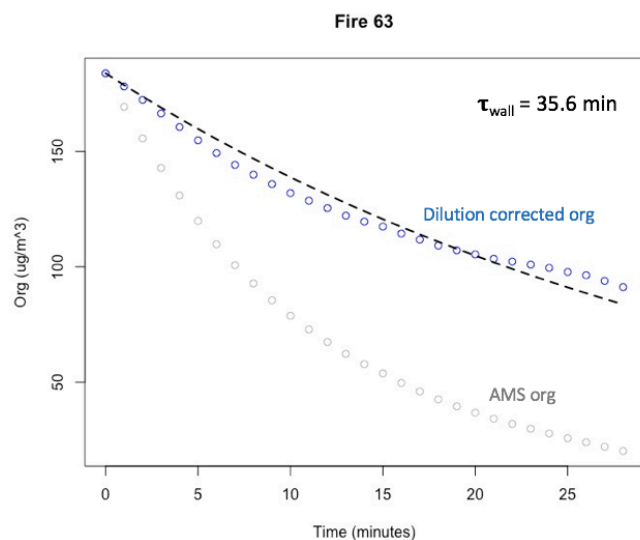
Figure S4. Wall loss fit for dark experiment (Fire 63). Wall loss time constant equals 35 minutes, based on fit of dilution corrected OA mass.

S5. Dilution corrected primary IVOCs
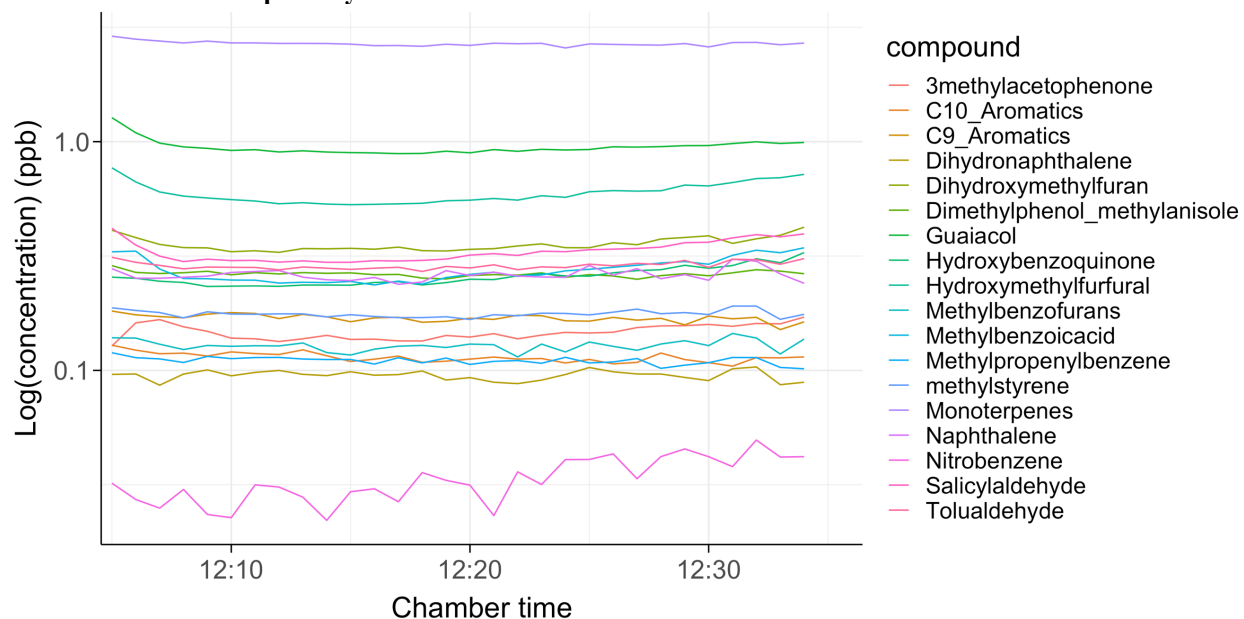
Figure S5. Time series for dilution-corrected, high molecular weight gas phase compounds measured by PTR-ToF-MS. Dilution corrected concentrations are stable, indicating the impact of vapor wall loss for these compounds is not important.

S6. Comparison between previous FSL aging studies
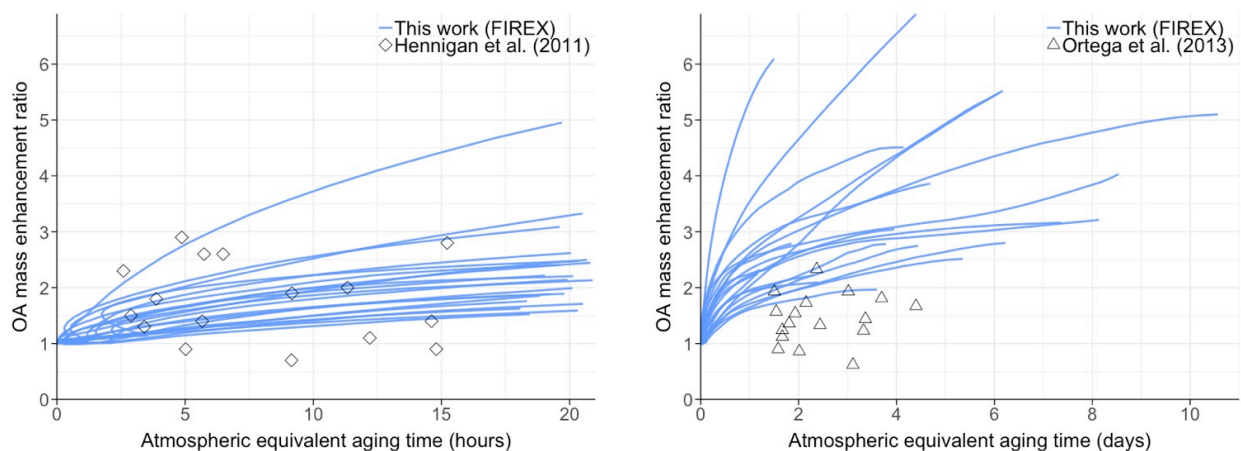
Figure S6. Comparison between OA enhancement ratios for this work and previous Fire Lab aging studies. Panel on left is comparison to room-burn, large chamber oxidation from Hennigan et al. (2011). Recent work from Ahern et al. (2019) is also roughly consistent with this, but includes an internal CE correction. Panel on right is comparison to room-burn, flow tube oxidation from Ortega et al. (2013). Data are not corrected for AMS collection efficiency in order to compare with published work (CE = 1).

S7. OA enhancement ratio scatterplots
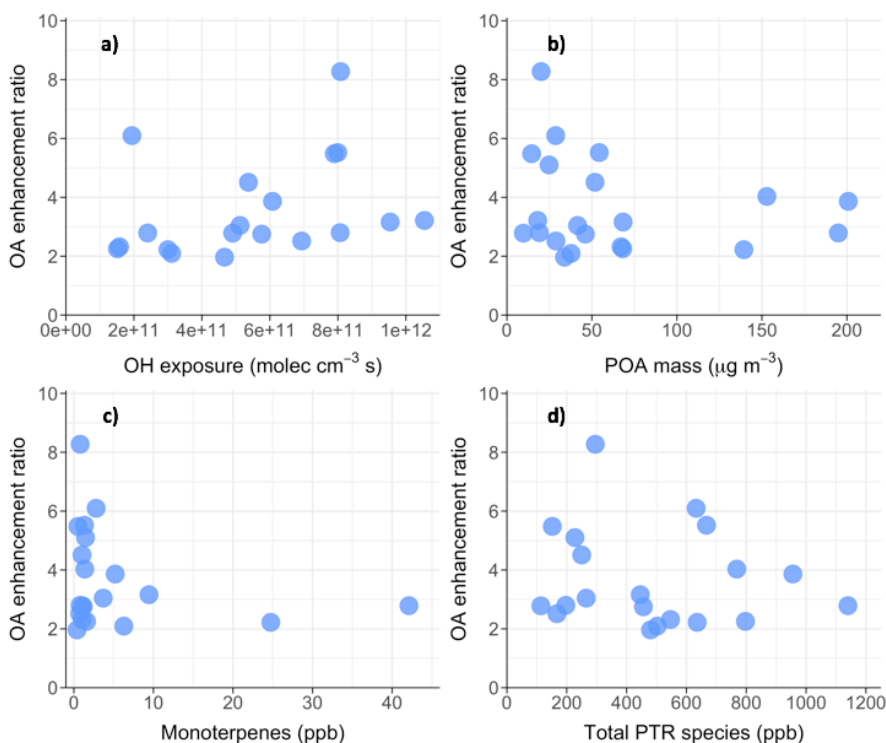
Figure S7. Scatterplots of OA enhancement ratio vs. various parameters: (a) OH exposure, (b) POA mass, (c) monoterpene concentration, (d) total PTR species. No single parameter shows a strong relationship with OA enhancement ratio.

S8. Effect of aerosol loading on carbon yield
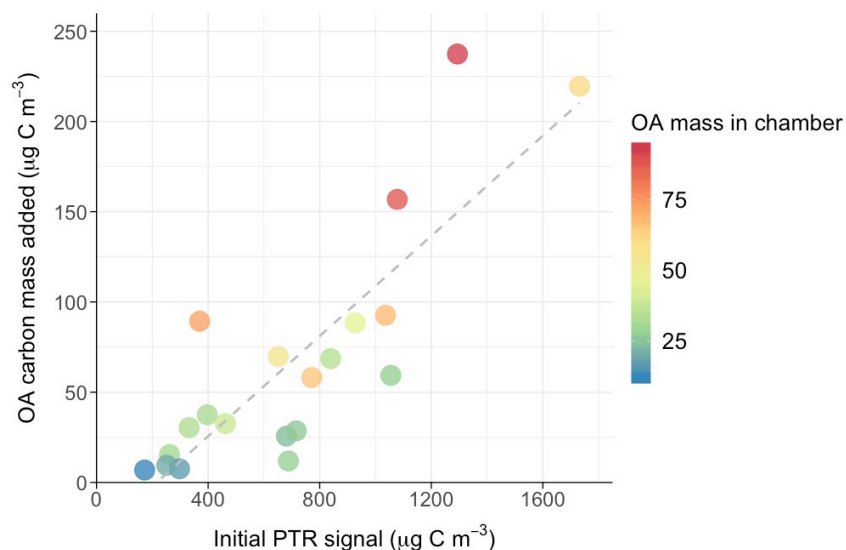
Figure S8. OA carbon mass added as a function of initial PTR signal and colored by OA mass in suspended in the chamber (1 day of equivalent exposure). Higher aerosol mass in the chamber contributes to higher conversion of gas-phase carbon to SOA.

S9. POA vs. SOA scatterplots
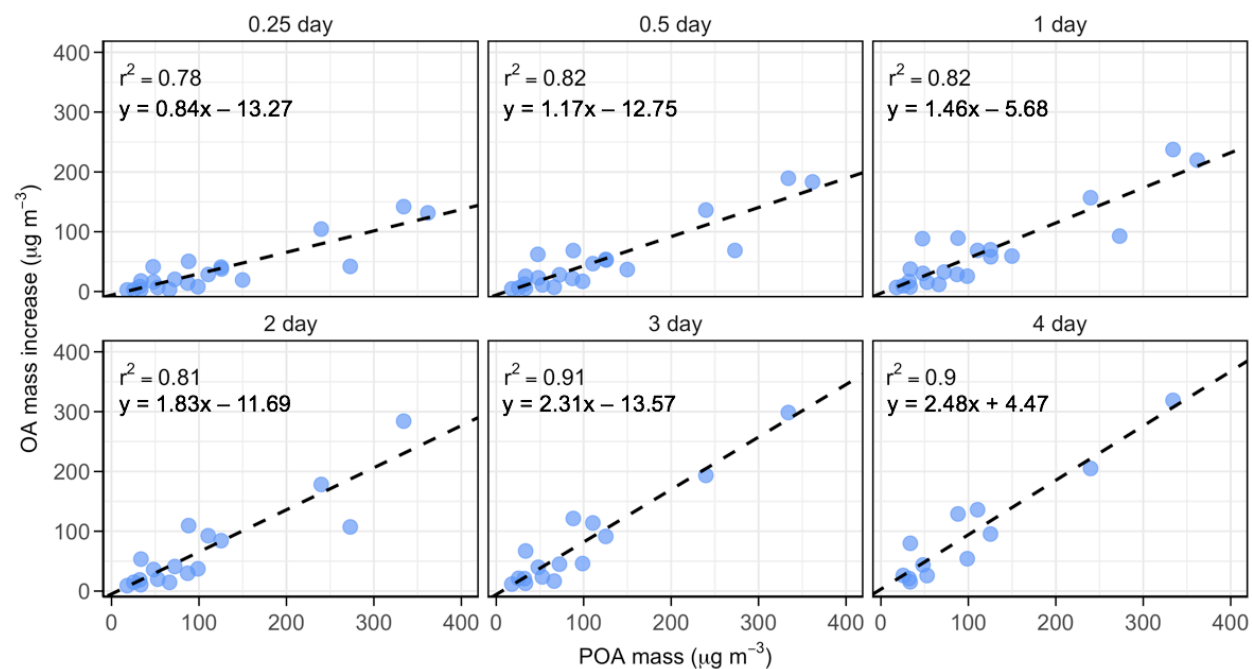
Figure S9. Scatterplots of SOA mass vs. POA mass at OH exposures equivalent to 0.25 days of atmospheric aging to 4 days of aging. Dashed lines are linear regressions described by the fit equations.